

Supplementary Information

Appendix 1: Detailed materials and methods

1.1 Irradiation apparatus. Experiments were conducted in an insulated room maintained at 28°C by an air conditioner (MSZ-VX28F-W, Mitsubishi Electric). A far infrared radiating heat source was positioned 14 cm above the bottom surface of FIR translucent culture flasks. The 2 × 1 m FIR panel was constructed from an aluminium sheet coated on both sides with ceramic composed of aluminium oxide (Al₂O₃, 87%) and titanium oxide (TiO₂, 13%) (Misato Plaheat Mfg., Ltd.). A thermostatically controlled electric heater warmed the panel, whose surface was maintained at 40°C (C-5113 Thermo Controller, Misato Plaheat) (Fig. 1). Wavelengths of noncoherent FIR emitted from the ceramic ranged from 3 to 25 μm with a broad peak at 10 μm. These values were determined by Fourier transform infrared spectroscopy (FT/IR-359, JASCO) of ceramic samples at 90°C (Fig. S1). Control flasks were incubated in an air convection incubator equipped with a fan that operated intermittently (CR-41, Hitachi).

Irradiance, the radiant power per unit area, was measured with a thin-foil planar radiometer (30 × 30 mm, Captec).¹⁵ This sensor was calibrated at 2.79 μV·W⁻¹·m⁻², connected to a μV signal amplifier (Captec) and digital multimeter (TR6846, Advantest), and inserted into one of the 25 cm², FIR translucent polystyrene culture flasks (430639, Corning)(Fig. S2). Under the panel, it registered 2.80 ± 0.04 W·m⁻² (mean ± SEM, *n* = 50). Inside the air convection incubator, it showed only 0.41 ± 0.01 W·m⁻² (mean ± SEM, *n* = 50).

1.2 Temperature regulation. Water temperatures inside and air temperatures outside sentinel flasks were recorded electronically (TR-71S, T&D Corp.) as matched pairs at

30 min intervals for 120 h of culture. Temperatures inside sentinel flasks were measured with waterproof sensors (TR-0306, T&D Corp.). Resin shielded sensors (TR-0106, T&D Corp.) logged air temperatures outside the flasks. One-way analysis of variance (ANOVA) showed random errors of the magnitude expected (Tables S1a, b).

1.3 Cell culture. *T. thermophila* SB1969 was inbred heterokaryon strain B, genotype *chx1-1/chx1-1*, phenotype cy-s and mating type II.^{2s} SB210 was heterokaryon strain B, genotype *gall-1/gall-1*, phenotype gal-s and mating type VI. Stationary phase stock cultures were maintained at 25°C in 0.25% (w/v) proteose peptone no. 3 (0122-17, Difco Laboratories), 0.25% (w/v) yeast extract (0127-17-9, Bacto[®] Laboratories) and 3.5% (w/v) dextrose (044-00605, Wako). Cell cultures were made with nonbuffered medium containing 1% proteose peptone, 0.5% yeast extract and 0.9% dextrose (PYD). Culture pH, monitored by a compact Twin pH meter (B-212, Horiba), rose from 6.8 to 8.3 during the growth cycle as ammonia and other waste products accumulated.

To measure cell concentration, cells from three independent 5 ml cultures were pooled. Then, appropriate dilutions of 50 µl samples were fixed in 4% (v/v) formalin, 0.001% (w/v) brilliant green dye. At least 1000 cells were counted using a haemocytometer (Fig. S3A-C). To prevent heat shock, cells from a log phase culture at 33°C in an air convection incubator were diluted to 1.0×10^4 cells ml⁻¹ in pre-warmed medium. Aliquots (5 ml) were transferred to 25 cm², FIR translucent polystyrene culture flasks (430639, Corning). Flasks were randomly assigned to FIR and control groups and incubated at 33°C undisturbed in the dark. Water lost to evaporation (250

μl) and that removed for counting (150 μl) was replaced daily. Vital Apofluor stain for apoptosis showed no evidence of programmed cell death.^{3s}

1.4 DNA isolation. Macronuclear DNA was extracted by a microtechnique based on established methods.^{4s} FIR treated SB1969 cells and controls were harvested at 24, 48 and 72 h of culture. In each experiment, three independent cultures were pooled, and DNA was extracted from samples of 1.0×10^6 cells. Cell culture suspensions were centrifuged in 1.5 ml Eppendorf[®] tubes at $2000 \times g$ for 3 min, and all but the last 50 μl of supernatant was removed. Cell pellets were resuspended by flicking the tube and adding 1 ml of ice-cold 10 mM Tris-HCl pH 7.5 containing 250 mM sucrose, 10 mM CaCl₂, 0.2% (v/v) NP-40 and 100 mM 2-mercaptoethanol.^{5s} Plasma membranes were disintegrated by vortex mixing the suspension for 30 sec. Fluorescence microscopy of 20 μl volumes stained with Hoechst 33342 (H-3570, Molecular Probes) confirmed that lysis was complete. Then, macronuclei were collected by differential centrifugation at $2000 \times g$ for 6 min.

Pellets rich in macronuclei were resuspended in 1 ml of 10 mM Tris-HCl pH 8.0 containing 10 mM NaCl, 23 mM EDTA, 100 mM 2-mercaptoethanol and 100 mM sodium para-aminosalicylate (A3505, Sigma).^{4s,6s} DNase-free RNase A (312-0193, Wako) was added to a final concentration of $10 \mu\text{g ml}^{-1}$, and tubes were incubated for 1 h at 37°C. Digests were made 300 mM in sodium para-aminosalicylate and divided into two tubes using large bore micropipette tips to minimize shearing of DNA.^{7s,8s} Then they were extracted twice with an equal volume of phenol, which had been equilibrated with the same buffer, and twice with chloroform. In each step, tubes were rotated at 20 rev min^{-1} for 20 min at 4°C. After chloroform extraction, the aqueous

phases were recombined, made 70% (v/v) in ethanol, and incubated overnight at -20°C . High molecular weight DNA precipitates were recovered by centrifugation at $15,000 \times g$ for 10 min at 4°C . Pellets were washed with 70% ethanol, air-dried and dissolved in 100 μl of 1 mM Tris-HCl pH 8.0, 0.1 mM EDTA for 48 h at 4°C .

To measure DNA concentration, triplicate aliquots from each isolate were diluted five fold in water for measurement by UV spectrophotometry (GeneSpec I, Naka Instruments). Mean DNA concentration was calculated from the absorbances at 260 nm (A_{260}) and the dilution factor, assuming that the absorbance of 1 unit at 260 nm corresponded to 50 μg of DNA ml^{-1} . Then mean DNA content in pg cell^{-1} was determined from the absorbances at 260 nm (A_{260}) and cell counts. ANOVA was done to compare FIR treated SB1969 cells and controls (Fig. S3D; Tables S4a-c).

Purity of the isolates was estimated from the UV absorbance ratios, A_{260}/A_{280} , A_{260}/A_{270} and A_{260}/A_{230} . DNA integrity was checked by electrophoresis in a 0.7% (w/v) LO3 agarose gel made with 89 mM Tris-borate, 2 mM EDTA. Before the run, each sample (0.2 μg) was dissolved in 7 μl of water, and 2 μl of loading dye was added. Additional samples were heated for 5 min at 65°C and chilled on ice to verify the formation of hairpin structures by denatured ribosomal DNA. *Hind* III digested Lambda phage DNA served as a molecular size marker. After electrophoresis, gels were stained in ethidium bromide (0.5 $\mu\text{g ml}^{-1}$), destained in water, and DNA bands were photographed by UV transillumination (Fig. S4).

1.5 RNA isolation. To extract total RNA, FIR treated SB1969 cells and controls were harvested at 24, 48 and 72 h of culture. In each experiment, cells from three independent cultures were pooled. Total RNA was extracted and affinity-purified

from samples of 3.0×10^6 cells using an RNeasy Mini Kit (74103, QIAGEN). Then, the isolates were treated with RNase-free DNase I, extracted with phenol/chloroform (3:1) and precipitated in ethanol with a Message Clean Kit (M601, GenHunter® Corp.). Triplicate aliquots from each isolate were diluted in water and measured by UV spectrophotometry (GeneSpec I, Naka Instruments). To ensure significance, dilutions were made so that the readings were greater than 0.15. Mean RNA concentration was calculated from the absorbances at 260 nm (A_{260}) and the dilution factor, assuming that the absorbance of 1 unit at 260 nm corresponded to 40 μg of RNA ml^{-1} . RNA integrity was checked by gel electrophoresis in 1% (w/v) agarose-MOPS-formaldehyde at pH 6.7 using total RNA from adult mouse liver as a standard.

1.6 Differential display. Reverse transcription polymerase chain reactions (RT-PCRs) for differential display were carried out using first-strand complementary DNA (cDNA) synthesized from isolates of total RNA, ExTaq DNA polymerase (RR001B, Takara Biomedicals), single base-anchored 3' primers (H-dT₁₁-A, -G or -C), and arbitrary 5' primers H-AP1-4 (GenHunter® Corp.).^{9s} Preparation of total RNA is described in Appendix 1.5, and PCR programmes are listed in Appendix 1.8. After electrophoresis in 6% (v/v) polyacrylamide gels, double-stranded cDNA bands were visualized with the fluorescent intercalating dye, SYBR Green I (S-7563, Molecular Probes). Gels were scanned using an FX External Laser Molecular Imager (Bio-Rad)(Fig. S5A). Slices containing selected bands were excised into 100 μl of 2X PCR buffer (M190G, Promega), and the solution was heated at 94°C for 90 min to elute the cDNA.^{10s} Then, the cDNAs were reamplified for *E. coli* JM109 competent cell transformation, colony PCR and sequencing by dideoxy chain termination using a

Thermo Sequenase™ Dye Primer Manual Cycle Sequencing Kit (79260, USB)(Fig. S5B).

1.7 Real time RT-PCR. Polymerase chain reactions with specific primers were monitored in real time by the iCycler iQ optical detection system version 3.0a (Bio-Rad). First-strand cDNA templates were synthesized from 1 µg of DNase I-treated total RNA using Omniscript reverse transcriptase (205111, QIAGEN) and a custom made oligo-dT₁₈ primer. The primer, designated BKXdT18, had the sequence 5'-GGATCCGGTACCTCGAGTTTTTTTTTTTTTTTTTTT-3'. Negative controls contained no reverse transcriptase. Preparation of total RNA is described in Appendix 1.5, and PCR programmes and primers are listed in Appendices 1.8 and 1.9. ExTaq DNA polymerase, which has 3' to 5' exonuclease activity, ensured high fidelity amplification.

Reactions were carried out in 20 µl volumes containing 1X ExTaq buffer, 2 mM Mg²⁺, 0.5 units of ExTaq, 200 µM dNTPs, 500 nM of forward and reverse primers, 0.25X SYBR Green I and 1 µl of 1:5 diluted first-strand cDNA template.

Experimental and control cDNA amplifications were measured in real time using specific oligonucleotide primers designed as described in Appendix 1.9. Negative controls lacking template also were included. Then, a mean index of relative abundance, abbreviated F/C to stand for the ratio of mRNA in FIR treated cells to controls, was estimated from the fold difference, $R^{\Delta C_t}$. ^{11s,12s} R was the amplification rate, the inverse logarithm of the slope in the log linear phase of the reaction. The measured value of R was 1.9 fold cycle⁻¹, and differences in mean rates of paired reactions were not significant. Ct was the mean threshold cycle of real time RT-PCR

determined from the points at which SYBR Green I fluorescence exceeded an arbitrary baseline. C_t is inversely proportional to the initial number of target sequences.^{13s}

ΔC_t was the mean C_t of the control group minus that of the FIR treated group.

Variations in C_t values between and within groups were calculated by ANOVA (Tables S5a-d).

1.8 PCR programmes. For differential display with random arbitrary primers, PCR amplification of reverse transcribed cDNAs was done in a T3 Thermocycler (Biometra®).^{9s} Single base-anchored downstream 3' primers were H-dT₁₁-A, -G or -C, where H stands for AAGCTT, the *Hind* III restriction site. Upstream 5' arbitrary primers (AP) were H-AP1, 5'-AAGCTTGATTGCC-3'; H-AP2, 5'-AAGCTTCGACTGT-3'; H-AP3, 5'-AAGCTTTGGTCAG-3' and H-AP4, 5'-AAGCTTCTCAACG-3' (H-AP primer set 1, GenHunter® Corp.). Reactions were carried out in nuclease-free clear plastic PCR tubes with dome shaped caps (430-01X-NBZ-Q, QSP® Porex Bio Products Inc.). Each tube contained 2 µl of first-strand cDNA, 2.5 µl of arbitrary primer H-AP- #, 1.0 µl of H-dT₁₁-A, -G or -C, 0.5 µl of dNTPs (2.5 mM), 1.0 µl of 10X ExTaq buffer, 0.05 µl of ExTaq polymerase (5 units µl⁻¹, Takara Biomedicals) and 2.95 µl of water. The programme began with one cycle of denaturation (95°C, 5 min), annealing (42°C, 2 min) and extension (72°C, 1 min), which was followed by 25 cycles of denaturation (95°C, 30 sec), annealing (42°C, 1 min) and extension (72°C, 30 sec).

For real time RT-PCR with specific primers, the programme began with preheating (94°C, 3 min), which was followed by 40 cycles of denaturation (94°C, 1 min), annealing (58°C, 45 sec) and extension (72°C, 1 min). A DNA melting analysis

programme then characterized the products. Reaction products, primers and DNA size markers were resolved by Mupid-2[®] electrophoresis in TBE buffer (90 mM Tris-borate, 2mM EDTA, pH 8.0) at 100 V in 3% (w/v) NuSieve 3:1 agarose gels (FMC Bioproducts). DNase I treated total RNAs also were tested for residual DNA contamination. A negative control containing all components of the first-strand cDNA synthesis reaction except reverse transcriptase enzyme was included in each gel. After electrophoresis, DNA bands were stained with ethidium bromide (0.5 µg ml⁻¹, 40 min) and photographed using UV transillumination.

1.9 Specific PCR primers. Twenty-seven highly conserved ‘housekeeping mRNAs’ were selected from forty-three candidates in the *Tetrahymena* Genome Database (<http://www.ciliate.org/genomeproj.shtml>). In the following list of primer sequences, GenBank accession numbers are shown in parentheses. Sequences are oriented 5′ to 3′ reading from left to right. Positions in the mRNA coding sequence that correspond to the first (leftmost) nucleotide in the forward or reverse primer are enumerated. A plus or minus sign indicates the plus strand or its complementary sequence. Internet programmes, (<http://alces.med.umn.edu/websub.html>) and (http://www-genome.wi.mit.edu/cgi-bin/primer/primer3_www.cgi), were used to design the oligonucleotide primer sequences. All primer sequences were checked for homology, GC content, melting temperature and the absence of palindromes using Genetyx-Win version 5.0. Then, they were synthesized and purified (DATE Concept). PCR with each primer set showed a single product of the expected length that was characterized by DNA melting and electrophoretic mobility.

For DNA polymerase to elongate a polynucleotide strand during PCR, it is critical that the 3' sequences of the primers match the template exactly. Therefore, to ensure specific amplification, primers for histone variants H2A.Z (hv1) and HHT3 (hv2) had 3' terminal nucleotides that did not match the coding sequences of their nonvariant counterparts. Conversely, primers for corresponding nonvariant histones HTA1-2 and HHT1-2 had 3' terminal nucleotides that did not match the variant sequence.

Specific primer sequences

ACT	Macronuclear Actin (M13939)	
Forward 600+	AAGGTTACGCTCTTCCTCACG	21-mer
Reverse 900-	ATGAAGGCAGGCTTGAAGAGG	21-mer
CaM	Calmodulin (X52242)	
Forward 119+	CCAAGGAATTGGGTACTGTCATG	23-mer
Reverse 319-	CATCTCTATCGAAGACCTTGAAGG	24-mer
CS/14FP	Citrate Synthase/14 nm Filament Protein (D90117)	
Forward 560+	CGACGAAGGTAAGATCTCCAAG	22-mer
Reverse 1060-	TCTCTCAAGACAGCGTGTCCG	21-mer
CyP1	Starvation Responsive Cysteine Protease (L03212)	
Forward 396+	TTGGAGAACAAAAGGTGCTG	20-mer
Reverse 595-	GCCATCCTCCTTTACATCCA	20-mer
DYH4	Ciliary Outer Arm Dynein Beta Heavy Chain (AF072878)	
Forward 12251+	CCGTCTTTTCCTTTCTGCTG	20-mer
Reverse 12483-	CCTTAGGTCCAAAACGACGA	20-mer
EF-1a	Elongation Factor-1 alpha, <i>T. pyriformis</i> (D11083)	
Forward 587+	CCCTTCATCCCCATCTCTG	19-mer
Reverse 1087-	GTGAGCAGTGTGGCAATCC	19-mer
GAP-C	Glyceraldehyde-3-Phosphate Dehydrogenase (AF319450)	
Forward 307+	TTGAAGGGTGGTGCTAAGAAGG	22-mer
Reverse 807-	ACCCAAGATACCCTTGAGTTCAC	23-mer
HAT-A1	Histone Acetyltransferase A Catalytic Subunit (U47321)	
Forward 29+	ATGCATAGAATGCAGCACCA	20-mer
Reverse 242-	GGCATT TTTGGCAACTAACG	20-mer

HHF1-2	Histones H4-I (X00417) and H4-II (10816)	
Forward 37+	GTCGGAGCCAAGAGACACTC	20-mer
Reverse 238-	TTCTTCTGGCGTGTTTCAGTG	20-mer
HHO1	Histone H1 (M14854)	
Forward 277+	AAGAGACCCGCTAAGGAAGC	20-mer
Reverse 475-	TGGAGCTCTTCTTGGCATCT	20-mer
HHP1	Heterochromatin Associated Protein 1-Like Protein (AF079405)	
Forward 172+	AGCAATGATAAACCTTAGACACCCA	25-mer
Reverse 352-	GAATTCCTTCACTGGATCTAATGC	25-mer
HHT1-2	H3 Histones (M87304) and (M87504)	
Forward 81+	AAAGTCTGCCCCCGC	15-mer
Reverse 278-	AGAGCAAGAACGGCAGAA	18-mer
HHT3	Histone H3.3 Replacement Variant hv2 (M87305)	
Forward 92+	CCGTCTCTGGTGGTGTC	17-mer
Reverse 279-	GAGGGCAAGGATAGCTTGG	19-mer
HMB-B	High Mobility Group B Chromatin Protein (M63425)	
Forward 218+	AGGAAAAGGCCACCTACGAT	20-mer
Reverse 417-	GGGAGCCTTCTTATCGTCCT	20-mer
HMG-C	High Mobility Group C Chromatin Protein (M63424)	
Forward 12+	CAAGAGACCCTTATCCGCTTT	21-mer
Reverse 211-	AGGCTTACAGTGCCTTTTCG	20-mer
HSP70	Heat Shock Protein 70 (AY028633)	
Forward 835+	ATTCTTTCTTCGAGCGCAAT	20-mer
Reverse 1040-	CTCGAACCTCCAACGAGAAC	20-mer
HSP82	Heat Shock Protein 82 (AF151114)	
Forward 870+	TTGGGAAGAACAATAAGCTGTCA	23-mer
Reverse 1370-	TCTTTCATTCTGGAGACGTAGTCC	24-mer
HTA1-2	Histones H2A.1 (L18892) and H2A.2 (L18893)	
Forward 61+	TCTAGATCCGCTAGAGCTGG	20-mer
Reverse 345-	GTTGGGTAAGACACCACCAT	20-mer
H2A.Z	Histone H2A Variant formerly called hv1 (X06725)	
Forward 23+	GTAAAGTCGGAGGCGCC	17-mer
Reverse 270-	GAGCAAGTGACGAGGAGT	18-mer
HTB1-2	Histone H2B.1 (10812) and H2B.2 (X05544)	
Forward 123+	AAAGCAAGTCCACCCTGATG	20-mer
Reverse 322-	AGATGGCGTGTCTAGCGAGT	20-mer

P80	Telomerase Associated Protein p80 (U25641)	
Forward 39+	CGAAAAATTGTGGTGGGAAC	20-mer
Reverse 242-	GGATCAGACTCAGCCACCTC	20-mer
RAD51	Homologous Recombination DNA Repair Enzyme (AF064516)	
Forward 413+	TACCCAAGGAAAAGGGTGGT	20-mer
Reverse 605-	AAAGCAGCAGCCTGGACTAA	20-mer
RPB2	RNA Polymerase II Subunit 2 (U46561)	
Forward 4+	AGAGGTCCAGTTGTAGCAATTGTC	24-mer
Reverse 304-	GAATAAGTTGCTTAGCTGCATATGG	25-mer
TERT	Telomerase Reverse Transcriptase (AF061652)	
Forward 2380+	GGAGTCCTTTGCTCATTTTACTTTG	25-mer
Reverse 2880-	CTATCTGCAAAGACCCTCAAAGA	24-mer
THD1	Histone Deacetylase (AF276431)	
Forward 70+	GATGAGACCATTGGATCGTACAA	23-mer
Reverse 270-	CAATTTCGATGTATTCGTCAGAGTG	24-mer
TUF11	Ubiquitin-Ribosomal Protein Fusion Protein †(10935)	
Forward 14+	CCCCAAAGCTACCAACTGC	19-mer
Reverse 214-	GCCTGCTGTGGCGATAATT	19-mer
† <i>T. thermophila</i> homolog of <i>T. pyriformis</i> .		
TWI1	Piwi related protein (AB084111)	
Forward 1788+	CGGTGTTGGTGAAGGCTAAT	20-mer
Reverse 1950-	CACATTCCCATCTTGGCTTT	20-mer

1.10 Histone isolation. Macronuclear histone proteins were isolated using a microtechnique based on established methods.^{14s} FIR treated SB1969 cells and controls were harvested at 24, 48 and 72 h of culture. In each experiment, cells from three independent cultures were pooled. Histone proteins were extracted from samples of 5.0×10^6 cells at 4°C in the presence of protease inhibitors (P8340, Sigma). In brief, two 1.5 ml Eppendorf® tubes, each containing 2.5×10^6 cells, were centrifuged at 2000 × g for 3 min. The supernatants were discarded, and macronuclear lysates were made from the pellets as described in Appendix 1.4. Lysates were incubated for 90 min with 500 units ml⁻¹ of DNase I and 10 µg ml⁻¹ of RNase A in 10 mM Tris-HCl, pH 7.5

containing 10 mM MgCl₂ and 5 mM CaCl₂. Digests were made 100 mM in 2-mercaptoethanol, 50 mM in EDTA and 150 mM in sodium para-aminosalicylate, and they were incubated for 30 min more. Then, proteins were extracted with 0.4 N H₂SO₄ for 60 min, and tubes were centrifuged at 15,000 × g for 10 min to remove insoluble debris. Acid soluble histones were precipitated from the supernatant by adding 100% (w/v) trichloroacetic acid to a final concentration of 20%. Precipitates were centrifuged as before to collect them in a single tube, and they were washed with acidified acetone (0.1% HCl) followed by acetone. Air-dried histone enriched proteins were dissolved in 150 μl of water by heating for 2 min at 100°C.

1.11 Immunoblots. Triplicate aliquots from each histone preparation were diluted five fold, and concentrations were measured in the range 0.1 to 2.0 mg ml⁻¹ by the *DC* protein assay (500-0111, Bio-Rad). Calf thymus histones (100725, ICN Biochemicals) were used as a standard. Based on these results, 2 μg were loaded per lane and resolved by SDS-PAGE in a 12 % (v/v) separating gel that employed a 3.9% (v/v) stacking gel. Calf thymus histone H3, which has two distinct isoforms, served as a positive control.^{15s} The outermost lanes contained nine molecular weight standards ranging in size from 6.5 to 200 kDa (161-0317, Bio-Rad). Proteins were tank-transferred to PVDF membranes at 14 constant volts overnight at 4°C in 25 mM ethanolamine/glycine pH 9.5 containing 20% (v/v) methanol.^{16s} Immediately after transfer, the membrane was stained for 1 min with 0.2% (w/v) Ponceau S in 1% (v/v) acetic acid and destained with water to visualize the bands. Then it was dried for 1 h at 37°C. The gel was stained with Coomassie brilliant blue (G 250, ICN Biomedicals) and compared to an identically loaded gel that was processed in parallel but not

electroblotted. Standards greater than 95 kDa were the only bands visible in the gel after blotting. The absence of lower molecular weight bands suggested that the transfer efficiency of histone enriched proteins exceeded 90% as described.^{16s}

All membrane blocking and antibody probing steps were carried out at 4°C in the presence of protease inhibitors (P8340, Sigma). To prevent nonspecific binding of antibodies, the rewetted blot was incubated for 1 h in phosphate buffered saline (PBS) containing 5 % (w/v) nonfat dry milk and 0.05% (v/v) Tween 20. Rabbit primary antibodies were diluted in PBS, 0.5% nonfat dry milk, 0.005% Tween 20 and applied overnight. Three 20 min washes in PBS, 0.05% Tween 20 were done at 25°C. Then, antibodies that remained bound were targeted by immersing the blot for 4 h in a 1:5000 dilution of affinity-purified, peroxidase-conjugated goat anti-rabbit IgG (H+L) (111-035-003, Jackson ImmunoResearch). Washes were done as before, and antibody reactivity was recorded as chemiluminescence (SuperSignal West Pico 34080, Pierce) on X-ray film (MXJB-1, Kodak).

Primary antibodies were tested sequentially as follows: 1) anti-dimethyl H3K4 (07-030, Upstate); 2) anti-trimethyl H3K4 (ab8580, Abcam Ltd.); 3) anti-dimethyl H3K9 (07-212, Upstate); and 4) anti-trimethyl H3K9 (ab8898, Abcam Ltd.).^{17s-20s} All were diluted 1:2000. In this system, histones H3 and H2A comigrate independent of the polyacrylamide concentration.^{14s} Nevertheless, their sequences are highly divergent, so H2A is unlikely to crossreact with antibodies to the amino-terminus of H3. However, sequences encompassing H3K9 and H3K27 contain the tetrapeptide motif, ARKS. Thus, antibodies to K9 may crossreact to some extent with K27. Normal rabbit IgG (BMPRABP01, Cosmo Bio, LTD) or dilution buffer served as negative controls. Antibody complexes were eluted from the blot by gentle agitation in 0.2 M

glycine pH 2.5 containing 0.1% (w/v) SDS and 0.05% Tween-20 for 30 min at 25°C.

To ensure that signals were removed completely, the washed blot was incubated in chemiluminescent substrate solution and exposed to film according to the manufacturer's instructions. Then it was rinsed in PBS, re-blocked and probed with a different primary antibody.

1.12 Rationale for the immunoblotting procedure. Strongly basic proteins such as histones are near isoelectric neutrality at pH 8.3 in standard Tris/glycine/methanol tank-transfer buffer. In addition, methanol removes SDS from proteins when the SDS-PAGE gel is equilibrated in this buffer prior to blotting. The combined effect is a negligible efficiency of protein transfer. Therefore, to maximize the charge-to-mass ratio of histone proteins, we replaced the standard buffer with 25 mM ethanolamine/glycine pH 9.5 containing 20% methanol. Likewise, we did not equilibrate the gel in transfer buffer before setting up the apparatus. As a result, the transfer efficiency of histone enriched proteins appeared to exceed 90%.^{16s}

Nonfat dry milk is commonly used to block nonspecific binding of antibodies to blotted membranes, and it is superior to albumin and gelatin.^{21s} The casein lactoprotein fraction of milk contains several proteases including plasmin (fibrinolysin), cathepsin D and aminopeptidase, however.^{22s,23s} These proteases degrade antigens on the membrane as well as antibodies in solution. Antigen loss is directly proportional to the concentration of milk in the blocking solution and antibody dilution solution.^{24s} It is also proportional to the time these solutions are in contact with the membrane. As a result, otherwise weak signals may be abolished.

Plasmin, the major protease system in milk, its zymogen known as plasminogen and their activators are extremely heat stable.^{23s} By contrast, plasmin inhibitor and plasmin activator inhibitors are heat labile. Indeed, heating milk at 95°C to inactivate proteases results in higher rather than lower activity. Consequently, we used a mammalian protease inhibitor cocktail (P8340, Sigma) at 5 $\mu\text{l ml}^{-1}$ and incubations at 4°C to ensure that histones and antibodies were not degraded during immunoblotting. These precautions permitted multiple rounds of antibody probing and eluting without a significant decrease in chemiluminescent signal intensity (Fig. 4A).

1.13 MTT assay. FIR treated SB1969 cells and controls were harvested at 24, 48 and 72 h of culture. In each experiment, three independent cultures were pooled. Then, samples of 2.8×10^4 cells were assayed in triplicate for metabolic activity using an MTT assay that was statistically optimized for *Tetrahymena*.^{25s} This colourimetric test is based on chemical reduction of the yellow tetrazolium salt, MTT, to water insoluble crystals of the purple azo dye, formazan. Dimethyl sulfoxide dissolves the crystals *in situ*, and optical absorbance at 550 nm varies directly with the concentration of solubilized formazan. High absorbance implies high metabolic activity. Mean absorbance was calculated after subtraction of nonspecific background. Cells from a stationary phase stock culture at 25 °C were used as a zero time control (Fig. 5). The reduced pyridine nucleotide cofactor, NADH, is responsible for most of the reduction of MTT.^{26s} Current evidence suggests that the reaction is associated with enzymes of the endoplasmic reticulum, endosome/lysosome membranes and plasma membranes as well as mitochondria.

1.14 Microscopy. Cells were processed for transmission electron microscopy by standard practices (Fig. 2). For scanning electron microscopy (Fig. 6A, E, F and H), cells were washed three times in 50 mM HEPES, pH 6.9, 36 mM NaCl, 0.1 mM Mg Acetate, 1 mM KCl by centrifugation for 5 min at 600 x g. Then they were fixed in freshly mixed 100 mM sodium cacodylate buffer, pH 7.2, 2.5% (v/v) glutaraldehyde, 1% (v/v) osmium tetroxide for 1 h at 4°C.^{27s} Cells were washed again as before and dehydrated by 10 min incubations in a graded (35 to 100%) ethanol series before freeze-drying in *t*-butyl alcohol.^{28s,29s} Specimens were mounted on adhesive tape (Nisshin EM Co., Ltd.), coated with gold using an ion sputter (JEOL JFC-100E) and photographed with a scanning electron microscope (JEOL JSM-6390LV). For phase-contrast microscopy (Fig. 6B-D, G and I), samples of cell cultures were rapidly fixed in freshly mixed 2.5% (v/v) glutaraldehyde, 1% (v/v) osmium tetroxide.^{27s} The former crosslinked microtubules and other proteins. The latter bound unsaturated lipids, imparting a brownish-black colour to membranes. Thus, morphology was preserved, and cells were stained while avoiding a centrifugation step that might distort cell shape or damage cilia. Wet mounts were made on microscope slides by quickly applying a 22 × 22 mm cover slip to 15 µl of fixed cells. The edges of the cover slip were sealed with clear nail polish, and slides were stored at 4°C overnight to allow time for the membranes of cilia to blacken thoroughly. Then, images were recorded by phase-contrast microscopy using an Olympus CKX41 microscope equipped with a C-5060 Wide Zoom camera. Fig. S6 is an enlarged version of Fig.6.

1.15 Supplementary references.

- 1s E. Gaviot, P. Godts, S. Guths and D. Leclercq, Thin foil planar radiometers: application for designing contactless ΔT sensors, *Meas. Sci. Technol.*, 1996, **7**, 489-494.
- 2s E.P. Hamilton and E. Orias, Genetic crosses: Setting up crosses, testing progeny, and isolating phenotypic assortants, *Methods Cell Biol.*, 2000, **62**, 219-240.
- 3s S.S. Mpoke and J. Wolfe, Differential staining of apoptotic nuclei in living cells: application to macronuclear elimination in *Tetrahymena*, *J. Histochem. Cytochem.*, 1997, **45**, 675-683.
- 4s M.-F. Chau and E. Orias, An improved method to obtain high molecular weight DNA from purified micro- and macronuclei of *Tetrahymena thermophila*, *J. Euk. Microbiol.*, 1996, **43**, 198-202.
- 5s T. Mita, H. Shiomi and K. Iwai, Isolation of nuclei from exponentially growing *Tetrahymena pyriformis*, *Expl. Cell Res.*, 1966, **43**, 696-699.
- 6s S. Tas, Involvement of disulfide bonds in the condensed structure of facultative heterochromatin and implications on cellular differentiation and aging, *Gerontology*, 1978, **24**, 358-364.
- 7s K.S. Kirby, A new method for the isolation of deoxyribonucleic acids: Evidence on the nature of bonds between deoxyribonucleic acid and protein, *Biochem. J.*, 1957, **66**, 495-504.
- 8s R. Shiurba and S. Nandi, Isolation and characterization of germ line DNA from mouse sperm, *Proc. Natl. Acad. Sci. USA*, 1979, **76**, 3947-3951.
- 9s P. Liang and A.B. Pardee, Differential display. A general protocol, *Mol. Biotechnol.*, 1998, **10**, 261-267.

- 10s M.R. Frost and J.A. Guggenheim JA, Prevention of depurination during elution facilitates the reamplification of DNA from differential display gels, *Nucleic Acids Res.*, 1999, **27**, e6.
- 11s A. Gentle, F. Anastasopoulos and N.A. McBrien, High-resolution semi-quantitative real-time PCR without the use of a standard curve, *Biotechniques*, 2001, **31**, 502, 504-506, 508.
- 12s M.W. Pfaffl, A new mathematical model for relative quantification in real-time RT-PCR, *Nucleic Acids Res.*, 2001, **29**, e45.
- 13s R. Higuchi, C. Fockle, G. Dollinger and R. Watson, Kinetic PCR analysis: Real-time monitoring of DNA amplification reactions, *Bio/Technology*, 1993, **11**, 1026-1030.
- 14s E.A. Wiley, C.A. Mizzen and C.D. Allis, Isolation and characterization of *in vivo* modified histones and an activity gel assay for identification of histone acetyltransferases, *Methods Cell Biol.*, 2000, **62**, 379-394.
- 15s W.F. Marzluff Jr., L. Sanders, D. Miller and K.S. McCarty, Two chemically and metabolically distinct forms of calf thymus F3, *J. Biol. Chem.*, 1972, **247**, 2026-2033.
- 16s B. Szewczyk and L.M. Kozloff, A method for the efficient blotting of strongly basic proteins from sodium dodecyl sulphate-polyacrylamide gels to nitrocellulose, *Anal. Biochem.*, 1985, **150**, 403-407.
- 17s B.D. Strahl, R. Ohba, R.G. Cook and C.D. Allis, Methylation of histone H3 at lysine 4 is highly conserved and correlates with transcriptionally active nuclei in *Tetrahymena*, *Proc. Natl. Acad. Sci. USA*, 1999, **96**, 14967-14972.

- 18s H. Santos-Rosa, R. Schneider, A.J. Bannister, J. Sherriff, B.E. Bernstein, N.C. Emre, S.L. Schreiber, J. Mellor and T. Kouzarides, Active genes are tri-methylated at K4 of histone H3, *Nature*, 2002, **419**, 407-411.
- 19s A.H. Peters, D. O'Carroll, H. Scherthan, K. Mechtler, S. Sauer, C. Schofer, K. Weipoltshammer, M. Pagani, M. Lachner, A. Kohlmaier, S. Opravil, M. Doyle, M. Sibilia and T. Jenuwein, Loss of the *SUV39h* histone methyltransferases impairs mammalian heterochromatin and genome stability, *Cell*, 2001, **107**, 323-337.
- 20s Q. Yan, J. Huang, T. Fan, H. Zhu and K. Muegge, Lsh, a modulator of CpG methylation, is crucial for normal histone methylation, *EMBO J.*, 2003, **22**, 5154-5162.
- 21s D.A. Johnson, J.W. Gautsch, J.R. Sportsman and J.H. Elder, Improved technique utilizing nonfat dry milk for analysis of proteins and nucleic acids transferred to nitrocellulose, *Gene Ana. Tech.*, 1984, **1**, 3-8.
- 22s M.J. Hurley, L.B. Larsen, A.L. Kelly and P.L.H. McSweeney, The milk acid proteinase cathepsin D: a review, *Int. Dairy J.*, 2002, **10**, 673-681.
- 23s S.S. Nielsen, Plasmin system and microbial proteases in milk: Characteristics, roles, and relationship, *J. Agric. Food Chem.*, 2002, **50**, 6628-6634.
- 24s N. DenHollander and D. Befus, Loss of antigens from immunoblotting membranes, *J. Immunol. Meth.*, 1989, **122**, 129-135.
- 25s N. Dias, A. Nicolau, G.S. Carvalho, M. Mota and N. Lima, Miniaturization and application of the MTT assay to evaluate metabolic activity of protozoa in the presence of toxicants, *J. Basic Microbiol.*, 1999, **39**, 103-108.

- 26s M.V. Berridge, P. M. Herst and A.S. Tan, Tetrazolium dyes as tools in cell biology: New insights into their cellular reduction, *Biotechnol. Ann. Rev.*, 2005, **11**, 127-152.
- 27s C.K. Omoto and C. Kung, Rotation and twist of the central-pair microtubules in the cilia of Paramecium, *J. Cell Biol.*, 1980, **87**, 33-46.
- 28s T. Inoue and H. Osatake, A new drying method of biological specimens for scanning electron microscopy: The t-butyl alcohol freeze-drying method, *Arch. Histol. Cytol.*, 1988, **51**, 53-59.
- 29s H. Akahori, H. Ishii, I. Nonaka and H. Yoshida, A simple freeze-drying device using t-butyl alcohol for SEM specimens, *J. Electron Microsc.*, 1988, **37**, 351-352.
- 30s K.M. Karrer, *Tetrahymena* genetics: Two nuclei are better than one, *Methods Cell Biol.*, 2000, **62**, 127-186.

Appendix 2: Supplementary tables

Statistical analyses of temperature (S1a, b), population doubling time (S2a), sexual conjugation (S2b, c), chromatin body size (S3a-d), macronuclear DNA content (S4a-c), real time RT-PCR (S5a-d), path length (S6a) and track linearity (S6b).

One-way analysis of variance, Fisher's exact test and Wilcoxon's nonparametric signed ranks test were used to compare data. Abbreviations: ANOVA, one-way analysis of variance; df, degrees of freedom; F, ratio of the mean square values defined as MS between groups divided by MS within groups; F crit, critical value of F at which the *P*-value equals or exceeds 0.050; M, mean; MS, mean square; *n*, sample size; *P*-value, probability that the observed difference in mean values is due to chance alone; SS, sum of the squares.

Table S1a Water temperature inside culture flask

Group	<i>n</i>	Sum	Mean	Variance
FIR	723	24198	33.5 °C	0.101
Control	723	24081	33.3	0.049

ANOVA

Variation	SS	df	MS	F	F crit	<i>P</i> -value
Between	9.4	1	9.40	126	3.85	< 0.0001
Within	108.0	1444	0.075			
Total	117.4	1445				

Water temperatures inside and air temperatures outside sentinel flasks were recorded electronically as matched pairs at 30 min intervals for 120 h of culture as described in Appendix 1.2. The small but significant difference in temperature variance inside the sentinel culture flasks was in accord with the fact that the FIR panel and control air convection incubator had separate thermostatic controllers. The data are representative of three independent experiments.

Table S1b Air temperature outside culture flask

Group	<i>n</i>	Sum	Mean	Variance
FIR	723	22362	30.9 °C	0.123
Control	723	24110	33.3	3.988

ANOVA

Variation	SS	df	MS	F	F crit	<i>P</i> -value
Between	2114.5	1	2114.5	1029	3.85	< 0.0001
Within	2967.6	1444	2.055			
Total	5082.1	1445				

Mean temperature of the air outside the control flask equalled that of the water inside (Table S1a). By contrast, mean temperature of the air outside the irradiated flask was 2.6°C lower than that of the water inside. The higher temperature inside the flask appeared to be evidence of an FIR induced greenhouse-like effect. The data are representative of three independent experiments.

Table S2a Population doubling time at 24 h of culture in mid-log phase

Group	<i>n</i>	Sum	Mean	Variance
FIR	80	5106	63.8 cells mm ⁻²	118.5
Control	80	5409	67.6	205.8

ANOVA

Variation	SS	df	MS	F	F crit	<i>P</i> -value
Between	574	1	574	3.54	3.90	> 0.050
Within	25620	158	162			
Total	26194	159				

SB1969 cells from a log phase pre-culture were diluted to 1.0×10^4 cells ml⁻¹ in prewarmed PYD medium containing 1% proteose peptone, 0.5% yeast extract and 0.9% dextrose. Cells were incubated for 24 h at 33°C. Triplicate 50 µl volumes were withdrawn, and cells were fixed in 50 µl of 4% formalin containing 0.001% brilliant green dye. Mean number of cells mm⁻² was determined using a haemocytometer. Mid-log phase doubling time (DT) was calculated using the formula $DT = (24 \log 2) \cdot (\log N - \log 10^4)^{-1}$, where N is the concentration in cells ml⁻¹ at 24 h. Both populations had a DT of 3.4 ± 0.1 h (mean \pm SEM, *n* = 80). The data are representative of five independent experiments.

Table S2b Tightly joined mating pairs of SB1969 and SB210 cells formed during 3.5 h

Group	<i>n</i>	Sum	Mean	Variance
FIR	48	2798	58.3 mp	236.2
Control	48	2667	55.6	142.3

ANOVA

Variation	SS	df	MS	F	F crit	<i>P</i> -value
Between	179	1	178.8	0.944	3.94	> 0.050
Within	17794	94	189.3			
Total	17973	95				

Mid-log phase cultures of heterokaryon strains SB1969 cells (genotype *chx1-1/chx1-1*, phenotype *cy-s*, type II) and SB210 (genotype *gal1-1/gal1-1*, phenotype *gal-s*, type VI) were diluted separately to 5×10^5 cells ml⁻¹ in NKC solution (0.2% NaCl, 0.008 % KCl and 0.012% CaCl₂). For starvation, 6 ml volumes were incubated overnight in 25 cm² flasks at 33°C. To begin costimulation, 2.5 ml from each initiated population were mixed and incubated under FIR and control conditions. After 3.5 h, triplicate 50 µl volumes were withdrawn using large bore micropipette tips. To disrupt newly formed homotypic and heterotypic pairs, which were morphologically indistinguishable, the suspensions were vortex mixed for 30 sec. Then, cells were added to 25 µl of 4% formalin, 0.001% brilliant green dye. Mean number of tightly joined mating pairs (mp) mm⁻² was determined using a haemocytometer. Tight pairs amounted to about 80% of the cells counted in each group. The data are representative of three independent experiments.

Table S2c Fertility—cycloheximide resistant progeny of single mating pairs

Group	Resistant	Sensitive	Row Total	P-value
FIR	174	15	189	0.152
Control	170	14	184	
Column Total	344	29	373	

Mid-log phase cultures of heterokaryon strains SB1969 cells (genotype *chx1-1/chx1-1*, phenotype cy-s, type II) and SB210 (genotype *gal1-1/gal1-1*, phenotype gal-s, type VI) were diluted separately to 5×10^5 cells ml⁻¹ in NKC solution (0.2% NaCl, 0.008 % KCl and 0.012% CaCl₂). For starvation, 6 ml volumes were incubated overnight in 25 cm² flasks at 33°C. To begin costimulation, 2.5 ml from each initiated population were mixed and incubated under FIR and control conditions. After 3.5 h, 1 ml of PYD culture medium was added for 1 h to separate young pairs and inhibit further pairing. Then, individual mating pairs were isolated using a manually pulled glass micropipette and transferred to 96-well plates. Each well contained a single-pair of cells in 200 µl of NKC. Nonpathogenic *Klebsiella pneumoniae* were suspended in the solution as a food source. The transfer procedure took 1 h. Plates were incubated in moist, FIR translucent chambers at 33°C under FIR and control conditions for 24 h more to allow cells to complete conjugation and proliferate. Wells without motile cells were marked for exclusion before the protein synthesis inhibitor cycloheximide (chx, 038-11131, Wako) was added to a concentration of 15 µg ml⁻¹. Two days later, plates were scored for drug phenotype by counting the number of wells with live (resistant) or dead (sensitive) cells. The P-value for this 2 × 2 contingency table was calculated by Fisher's exact test. cf. E.P. Hamilton and E. Orias, Genetic crosses: Setting up crosses, testing progeny and isolating phenotypic assortants, *Methods Cell Biol.*, 2000, **62**, 219-240. The data are representative of two independent experiments.

Table S3a Chromatin body size at 48 h of culture in early stationary phase

Group	n	Sum	Mean	Variance
FIR	1070	19795629	18500 nm ²	1.56×10^8
Control	1023	31790694	31076	3.87×10^8

ANOVA

Variation	SS	df	MS	F	F crit	P-value
Between	8.27×10^{10}	1	8.27×10^{10}	307	3.85	< 0.0001
Within	5.63×10^{11}	2091	2.69×10^8			
Total	6.45×10^{11}	2092				

After 48 and 72 h of incubation, three independent cultures of FIR treated SB1969 cells or controls were pooled. Samples were processed for transmission electron microscopy, and photographs were taken at a magnification of 10,000 and included a 500 nm scale bar. Images were scanned using Adobe Photoshop version 7.0. Then, chromatin body size was measured in nm² by a pixel counting macro programme for Scion Image software version 4.03. Each image was calibrated using its 500 nm scale bar, which corresponded to 62 pixels. In this format, one pixel equalled 8.06 nm, and one square pixel corresponded to an area of 65.03 nm². Images of five macronuclei selected at random from FIR treated cells or controls were analysed. The data are representative of three independent experiments.

Table S3b Chromatin body size at 72 h of culture in late stationary phase

Group	<i>n</i>	Sum	Mean	Variance
FIR	1168	27833480	23830 nm ²	2.82 × 10 ⁸
Control	1085	34785428	32060	4.55 × 10 ⁸

ANOVA

Variation	SS	df	MS	F	F crit	<i>P</i> -value
Between	3.81 × 10 ¹⁰	1	3.81 × 10 ¹⁰	104	3.85	< 0.0001
Within	8.22 × 10 ¹¹	2251	3.65 × 10 ⁸			
Total	8.60 × 10 ¹¹	2252				

Table S3c Comparison of irradiated chromatin body size at 48 and 72 h of culture

Group	<i>n</i>	Sum	Mean	Variance
FIR 48 h	1070	19795629	18500 nm ²	1.56 × 10 ⁸
FIR 72 h	1168	27833480	23830	2.82 × 10 ⁸

ANOVA

Variation	SS	df	MS	F	F crit	<i>P</i> -value
Between	1.59 × 10 ¹⁰	1	1.59 × 10 ¹⁰	71.6	3.85	< 0.0001
Within	4.96 × 10 ¹¹	2236	2.22 × 10 ⁸			
Total	5.11 × 10 ¹¹	2237				

Table S3d Comparison of control chromatin body size at 48 and 72 h of culture

Group	<i>n</i>	Sum	Mean	Variance
Control 48 h	1023	31790694	31076 nm ²	3.87 × 10 ⁸
Control 72 h	1085	34785428	32060	4.55 × 10 ⁸

ANOVA

Variation	SS	df	MS	F	F crit	<i>P</i> -value
Between	5.10 × 10 ⁹	1	5.10 × 10 ⁹	1.21	3.85	> 0.050
Within	8.89 × 10 ¹¹	2106	4.22 × 10 ⁸			
Total	8.89 × 10 ¹¹	2107				

Table S4a Macronuclear DNA content at 24 h of culture in mid-log phase

Group	<i>n</i>	Sum	Mean	Variance
FIR	27	735	27.2 pg cell ⁻¹	37.9
Control	27	611	22.6	112

ANOVA

Variation	SS	df	MS	F	F crit	<i>P</i> -value
Between	284.7	1	284.7	3.79	4.03	> 0.050
Within	3902	52	75.05			
Total	4188	53				

FIR treated SB1969 cells and controls were harvested at 24, 48 and 72 h of culture. Three independent cultures were pooled, and macronuclear DNA was extracted from triplicate samples of 1.0×10^6 cells. Then, triplicate dilutions of each extract were quantified by UV spectrophotometry, and picograms (pg) of DNA cell⁻¹ were calculated. All preparations were substantially free of contaminating RNA and protein ($A_{260}/A_{280} \cong 1.8$), phenol ($A_{260}/A_{270} \cong 1.2$) and 2-mercaptoethanol ($A_{260}/A_{230} \cong 2.0$). The data are representative of three independent experiments.

Table S4b Macronuclear DNA content at 48 h of culture in early stationary phase

Group	<i>n</i>	Sum	Mean	Variance
FIR	27	903	33.4 pg cell ⁻¹	83.6
Control	27	846	31.3	183

ANOVA

Variation	SS	df	MS	F	F crit	<i>P</i> -value
Between	60.17	1	60.17	0.451	4.03	> 0.050
Within	6933	52	133.3			
Total		53				

Table S4c Macronuclear DNA content at 72 h of culture in late stationary phase

Group	<i>n</i>	Sum	Mean	Variance
FIR	27	672	24.9 pg cell ⁻¹	89.0
Control	27	631	23.4	87.8

ANOVA

Variation	SS	df	MS	F	F crit	<i>P</i> -value
Between	31.12	1	31.12	0.352	4.03	> 0.050
Within	4597	52	88.40			
Total	4628	53				

Table S5a Real time RT-PCR of cDNA templates from cells at 24 h of culture

mRNA	Tm	FCt	FS ²	CCt	CS ²	ΔCt	P-value	F/C
ACT	87	16.6	0.08	16.5	0.20	-0.1	> 0.050	1.0
CaM	86	15.5	0.11	15.1	0.01	-0.4	> 0.050	1.0
CS/14FP	87	18.1	0.04	18.3	0.17	+0.2	> 0.050	1.0
CyP1	87	24.0	0.14	23.5	0.48	-0.5	> 0.050	1.0
DYH4	85	26.4	0.07	26.6	0.16	+0.2	> 0.050	1.0
EF-1a	91	13.8	0.08	14.2	0.12	+0.4	> 0.050	1.0
GAP-C	90	16.4	0.08	16.1	0.23	-0.3	> 0.050	1.0
HAT-A1	86	22.6	0.09	22.7	0.11	+0.1	> 0.050	1.0
HHF1-2	87	14.0	0.01	14.0	0.20	0.0	> 0.050	1.0
HHO1	89	14.6	0.13	14.6	0.05	0.0	> 0.050	1.0
HHP1	83	20.7	0.13	22.0	0.06	+1.3	< 0.001	2.3
HHT1-2	88	18.7	0.10	18.3	0.04	-0.4	> 0.050	1.0
HHT3	86	21.0	0.01	21.0	0.01	0.0	> 0.050	1.0
HMG-B	89	15.5	0.04	15.9	0.02	+0.4	> 0.050	1.0
HMG-C	86	13.9	0.05	13.3	0.12	-0.6	< 0.025	0.7
HSP70	84	23.3	0.16	24.5	0.25	+1.2	< 0.025	2.2
HSP82	88	19.9	0.09	20.5	0.20	+0.6	< 0.050	1.4
HTA1-2	88	14.1	0.05	14.0	0.02	-0.1	> 0.050	1.0
H2A.Z	88	12.4	0.05	12.3	0.03	-0.1	> 0.050	1.0
HTB1-2	88	13.5	0.10	13.1	0.03	-0.4	> 0.050	1.0
P80	85	28.2	0.09	28.1	0.01	-0.1	> 0.050	1.0
RAD51	86	18.5	0.23	18.0	0.14	-0.5	> 0.050	1.0
RPB2	87	20.0	0.01	19.9	0.16	-0.1	> 0.050	1.0
TERT	82	21.1	0.07	23.1	0.01	+2.0	< 0.001	3.6
THD1	84	27.6	0.25	27.6	0.36	0.0	> 0.050	1.0
TUF11	84	14.3	0.03	14.3	0.07	0.0	> 0.050	1.0
TWI1	82/87*	33.2	0.07	32.0	0.05	-1.2	< 0.001	0.5

In a preliminary survey of gene expression, mean relative abundance of mRNA in FIR treated SB1969 cells versus control was estimated as an F/C index after RT-PCR of total RNAs ($n = 5$). Shaded areas highlight mRNAs with F/C indices that fluctuated two fold or more. Technical details are in Appendices 1.7 to 1.9. Parameter abbreviations: Ct, the real time RT-PCR cycle number at which SYBR Green I fluorescence exceeds an arbitrary baseline and is inversely proportional to the initial number of target sequences; CCt, control threshold cycle; FCt, FIR treated threshold cycle; ΔCt, the CCt minus the FCt; F/C, estimated index of relative abundance that stands for the ratio of mRNA in FIR treated cells to controls; P-value, probability that the observed difference in FCt and CCt values is due to chance alone; S², statistical variance; Tm, mean melting temperature for the full-length PCR product.

mRNA abbreviations: ACT, macronuclear actin; CaM, calmodulin; CS/14FP, citrate synthase/14 nm filament protein; CyP1, cysteine protease; DYH4, ciliary outer arm dynein beta heavy chain; EF-1a, elongation factor 1 alpha; GAP-C, glyceraldehyde-3-phosphate dehydrogenase; HAT-A1, histone acetyltransferase A catalytic subunit; HHF1-2, core histones H4-I and H4-II; HHO1, linker histone H1; HHP1, heterochromatin associated protein 1-like protein; HHT1-2, H3 core histones; HHT3, macronuclear histone H3.3 replacement variant hv2; HMG-B, high mobility group B chromatin protein; HMG-C, high mobility group C chromatin protein; HSP70, heat shock protein 70; HSP82, heat shock protein 82; HTA1-2, core histones H2A.1 and H2A.2; H2A.Z, histone H2A variant formerly called hv1 (HTA3); HTB1-2, core histones H2B.1 and H2B.2; P80, telomerase associated protein p80; RAD51, homologous recombination DNA repair enzyme; RPB2, RNA polymerase II subunit 2; TERT, telomerase reverse transcriptase; THD1, *Tetrahymena* histone deacetylase; TUF11, ubiquitin ribosomal protein fusion protein; TWI1, piwi related protein (asterisk marks two Tm, consistent with alternative splicing of the mRNA by retaining the 65 nt intron 4).

Table S5b Real time RT-PCR of cDNA templates from cells at 48 h of culture

mRNA	Tm	FCt	FS ²	CCt	CS ²	ΔCt	P-value	F/C
ACT	87	16.8	0.08	16.3	0.09	-0.5	> 0.050	1.0
CaM	86	15.3	0.08	14.6	0.22	-0.7	< 0.025	0.6
CS/14FP	88	18.6	0.10	18.2	0.20	-0.4	> 0.050	1.0
CyP1	87	20.0	0.08	19.6	0.38	-0.4	> 0.050	1.0
DYH4	85	26.1	0.03	25.1	0.09	-1.0	< 0.001	0.5
EF-1a	91	14.1	0.01	13.4	0.02	-0.7	< 0.001	0.6
GAP-C	90	15.5	0.12	15.0	0.06	-0.5	> 0.050	1.0
HAT-A1	86	22.0	0.33	21.3	0.25	-0.7	> 0.050	1.0
HHF1-2	87	14.9	0.06	14.3	0.03	-0.6	< 0.005	0.7
HHO1	89	16.5	0.03	15.9	0.13	-0.6	< 0.025	0.7
HHP1	83	21.7	0.79	21.2	1.00	-0.5	> 0.050	1.0
HHT1-2	88	20.3	0.08	19.0	0.03	-1.3	< 0.001	0.4
HHT3	86	20.7	0.02	20.1	0.03	-0.6	< 0.001	0.7
HMG-B	89	15.9	0.10	15.5	0.03	-0.4	> 0.050	1.0
HMG-C	86	15.9	0.01	14.8	0.20	-1.1	< 0.001	0.5
HSP70	84	24.3	0.14	23.4	0.09	-0.9	< 0.005	0.6
HSP82	88	20.6	0.13	19.4	0.17	-1.2	< 0.005	0.5
HTA1-2	88	15.6	0.02	14.8	0.17	-0.8	< 0.005	0.6
H2A.Z	87	9.7	0.02	9.6	0.02	-0.1	> 0.050	1.0
HTB1-2	88	14.4	0.08	13.8	0.09	-0.6	< 0.005	0.7
P80	85	26.1	0.01	25.3	0.03	-0.8	< 0.001	0.6
RAD51	86	18.7	0.16	18.2	0.05	-0.5	> 0.050	1.0
RPB2	87	20.5	0.03	19.7	0.16	-0.8	< 0.001	0.6
TERT	82	23.1	0.14	23.2	0.01	+0.1	> 0.050	1.0
THD1	84	27.4	0.17	28.1	0.24	+0.7	> 0.050	1.6
TUF11	84	14.7	0.14	14.3	0.07	-0.4	> 0.050	1.0
TWI1	82/87*	32.1	0.05	31.1	0.04	-1.0	< 0.001	0.5

Table S5c Real time RT-PCR of cDNA templates from cells at 72 h of culture

mRNA	Tm	FCt	FS ²	CCt	CS ²	ΔCt	P-value	F/C
ACT	87	16.0	0.12	17.0	0.01	+1.0	< 0.001	1.9
CaM	86	15.0	0.12	16.9	0.06	+1.9	< 0.001	3.4
CS/14FP	88	18.9	0.15	22.3	0.23	+3.4	< 0.001	8.9
CyP1	87	18.7	0.04	19.0	0.23	+0.3	> 0.050	1.0
DYH4	85	24.5	0.01	27.3	0.05	+2.8	< 0.001	6.0
EF-1a	90	16.6	0.11	16.9	0.07	+0.3	> 0.050	1.0
GAP-C	90	16.2	0.01	18.0	0.21	+1.8	< 0.001	3.1
HAT-A1	86	23.3	0.02	22.9	0.09	-0.4	> 0.050	1.0
HHF1-2	87	15.6	0.05	16.9	0.04	+1.3	< 0.001	2.3
HHO1	89	17.9	0.09	20.9	0.20	+3.0	< 0.001	6.9
HHP1	83	21.9	0.14	21.9	0.60	0.0	> 0.050	1.0
HHT1-2	88	21.5	0.01	23.9	0.01	+2.4	< 0.001	4.7
HHT3	86	20.3	0.02	20.2	0.01	-0.1	> 0.050	1.0
HMG-B	89	16.7	0.02	19.3	0.16	+2.6	< 0.001	5.3
HMG-C	86	16.5	0.09	17.4	0.13	+0.9	< 0.005	1.8
HSP70	84	29.4	0.23	29.9	0.17	+0.5	> 0.050	1.0
HSP82	88	26.8	0.25	27.8	0.16	+1.0	< 0.010	1.8
HTA1-2	88	16.1	0.03	17.5	0.34	+1.4	< 0.005	2.5
H2A.Z	87	9.7	0.01	9.8	0.03	+0.1	> 0.050	1.0
HTB1-2	88	15.6	0.13	17.0	0.10	+1.4	< 0.001	2.5
P80	85	27.1	0.01	27.0	0.02	-0.1	> 0.050	1.0
RAD51	86	17.8	0.04	18.6	0.14	+0.8	< 0.005	1.7
RPB2	87	21.0	0.06	21.9	0.18	+0.9	< 0.005	1.8
TERT	82	28.5	0.32	27.6	0.06	-0.9	< 0.025	0.6
THD1	84	26.8	0.11	26.8	0.16	0.0	> 0.050	1.0
TUF11	84	14.5	0.07	13.8	0.05	-0.7	< 0.005	0.6
TWI1	82/87*	31.4	0.23	29.9	0.15	-1.5	< 0.001	0.4

Table S5d Normalized Threshold Cycles of cDNA Templates

24 h			48 h			72h		
mRNA	NF	NC	mRNA	NF	NC	mRNA	NF	NC
H2A.Z	100	100	H2A.Z	100	100	H2A.Z	100	100
HTB1-2	92	95	EF1a	69	72	TUF11	67	70
HMG-C	89	93	HTB1-2	67	70	CaM	65	57
HHF1-2	89	89	TUF11	66	68	HTB1-2	62	57
HTA1-2	88	89	HHF1-2	65	68	HHF1-2	62	57
EF1a	90	87	CaM	63	66	ACT	61	57
TUF11	87	87	HTA1-2	62	66	EF-1a	58	57
HHO1	85	85	HMG-C	61	66	HMG-C	59	56
CaM	80	82	GAP-C	63	65	HTA1-2	60	55
HMG-B	80	78	HMG-B	61	63	GAP-C	60	54
GAP-C	76	77	HHO1	59	61	RAD51	54	52
ACT	75	75	ACT	58	60	CyP1	52	51
RAD51	67	69	CS/14FP	52	54	HMG-B	58	51
CS/14FP	68	68	RAD51	52	53	HHT3	48	48
HHT1-2	66	68	HHT1-2	48	51	HHO1	54	47
RPB2	62	62	HSP82	47	50	CS/14FP	51	44
HSP82	62	60	CyP1	48	49	RPB2	46	44
HHT3	59	59	RPB2	47	49	HHP1	44	44
HHP1	60	56	HHT3	47	48	HAT-A1	42	42
HAT-A1	55	55	HHP1	45	46	HHT1-2	45	41
TERT	59	53	HAT-A1	44	46	DYH4	40	36
CyP1	52	52	TERT	42	42	THD1	36	36
HSP70	53	51	HSP70	40	41	P80	36	36
DYH4	47	47	DYH4	37	39	HSP82	36	35
THD1	45	45	P80	37	38	TERT	34	35
P80	44	44	THD1	35	34	HSP70	33	32
TWI1	37	39	TWI1	30	31	TWI1	31	32
Sum	1867	1865	Sum	1445	1496	Sum	1394	1326
W	3.5		W	-316		W	198	
n _{s/r}	14		n _{s/r}	25		n _{s/r}	21	
z	0.09		z	-4.24		z	3.43	
P-value	0.464		P-value	< 0.0001		P-value	0.0003	

Wilcoxon's nonparametric signed ranks test for two groups arranged as paired observations. Threshold cycles (Ct) from Tables S5a-c were normalized to the corresponding Ct of H2A.Z at each point. The F/C index for H2A.Z was 1.0 at all three points, and its Ct's were the lowest of the twenty-seven mRNAs examined. Assuming that Ct is inversely proportional to the starting number of target sequences, H2A.Z mRNA levels appeared to be predominant as well as temporally equivalent in experimental and control cells. As the supply of nutrients decreased, the relative abundance of mRNA for the starvation responsive cysteine protease gene *CyP1* increased in rank (shaded areas). It did not differ significantly in irradiated and control cells, however. Abbreviations: NC, normalized control Ct; NF, normalized FIR treated Ct; n_{s/r}, number of signed ranks; P-value, probability the observed differences are due to chance alone in a 1-tail test ($\alpha = 2, n = 27$); W, sum of the signed ranks; z, ratio which measures how far and in what direction an item differs from its distribution's mean, expressed in units of standard deviation. Statistics were calculated using VassarStats (<http://faculty.vassar.edu/lowry/wilcoxon.html>).

Table S6a Swimming path length at 72 h of culture in late stationary phase

Group	<i>n</i>	Sum	Mean	Variance
FIR	100	30382	304 μm	9072
Control	100	29779	298	20574

ANOVA

Variation	SS	df	MS	F	F crit	<i>P</i> -value
Between	1816	1	1816	0.122	3.89	> 0.050
Within	2934999	198	14823			
Total	2936814	199				

Table S6b Track linearity index at 72 h of culture in late stationary phase

Group	<i>n</i>	Sum	Mean	Variance
FIR	100	94	0.94	0.013
Control	100	77	0.77	0.080

ANOVA

Variation	SS	df	MS	F	F crit	<i>P</i> -value
Between	1.483	1	1.483	31.9	3.89	< 0.0001
Within	9.199	198	0.046			
Total	10.682	199				

Track linearity index was defined as the ratio of the start-to-finish linear distance to the actual swimming path length and was computed by a custom made programme for a Scion Image 4.03 macro file.

Supplementary figure legends

Fig. S1. Far infrared emission spectrum of the aluminium oxide/titanium oxide ceramic panel. A theoretical curve of black body radiation (black) is shown above wavelengths of noncoherent FIR (red) that range from 3 to 25 μm with a broad peak near 10 μm . These values were determined by Fourier transform infrared spectroscopy of ceramic samples at 90°C.

Fig. S2. Transmittance spectrophotometry of polystyrene composing the FIR translucent culture flask. The X-axis is a scale of energies in wavenumbers that are proportional to electromagnetic energy. The Y-axis, labeled % transmittance, is the ratio of the intensity of radiation transmitted through the sample compared to that of the incoming beam.

Fig. S3. Vegetative population growth (A-C) and macronuclear DNA content (D) of *T. thermophila* SB1969 cells left undisturbed in the dark at 33°C. Asynchronous growth did not differ significantly between irradiated and control cultures. At 24 h in mid-log phase, the doubling time was 3.4 ± 0.1 h (mean \pm SEM, $n = 80$) for both groups (Table S2a). (A) Cell concentration at 24 h intervals after inoculation with 1.0×10^4 cells ml^{-1} . At a surface-to-volume ratio of 5 to 1, a saturation density close to 2.75×10^6 cells ml^{-1} was attained by 48 h in early stationary phase. Then, the frequency of cell-to-cell collisions appeared to reach a maximum. Stationary phase lasted until 72 h, when population sizes began to decline about two fold. By 96 h, they were decimated, and most cells were undergoing autolysis. Only rare cells were alive at 120 h. Data are means \pm SEM of five independent experiments ($n = 80$). (B) Reciprocal exchange of

cells exposed to FIR or control conditions over four days before inoculation into fresh medium did not affect proliferation or saturation density. Data are means \pm SEM of three independent experiments ($n = 48$). (C) Reciprocal exchange of medium incubated under FIR or control conditions over five days before inoculation with cells did not change the doubling time. Saturation density decreased almost 30% in both groups, however. Prolonged incubation at 33°C rather than FIR itself appeared to reduce the nutrient value of the medium. The data are means \pm SEM of three independent experiments ($n = 48$). Technical details are in Appendix 1.3. (D) Macronuclear DNA content varied with the phase of population growth and did not differ significantly between FIR treated and control cells (Tables S4a-c). DNA content declined at 72 h when cells begin to starve and die. The data are means \pm SEM of three independent experiments ($n = 27$). Technical details are in Appendix 1.4.

Fig. S4. Assessment of SB1969 cell DNA integrity by agarose gel electrophoresis using *Hind* III digested Lambda phage DNA as a size marker. DNA bands were visualized by UV transillumination of an ethidium bromide stained gel. (A) Native 21 kb ribosomal DNA (rDNA) appeared as a single sharp band with an electrophoretic mobility near that of the 23.1 kb Lambda *Hind* III fragment. A slower migrating, diffuse band of bulk nuclear DNA was located nearby. (B) Denaturing the double-stranded DNA by heating caused the sharp band to shift to *ca.* 10.5 kb. The shift was predicted for nondegraded single-stranded macronuclear ribosomal DNA, whose sequence is a long inverted repeat.^{30s} After the strands separate, the head-to-head palindromic dimer folds back on itself, forming a hairpin motif. Technical details are in Appendix 1.4.

Fig. S5. Differential display reverse transcription polymerase chain reactions. (A) Double-stranded cDNA bands resolved by polyacrylamide gel electrophoresis. The upstream random arbitrary primers were H-AP1-4 (GenHunter[®] Corp.). The single base-anchored primer was H-T₁₁-A, where H stands for the *Hind* III restriction site, AAGCTT. The numbers 48 and 72 refer to hours of culture. F and C stand for FIR or control cDNAs. The large arrowhead at left points towards a cDNA band differentially increased at 72 h of culture in samples of FIR treated cells (72F). Small arrowheads point towards differentially expressed cDNAs with no exact matches in the GenBank database. The image is representative of three independent experiments. (B) Sequence of the 72F cDNA. Positions 5 to 295 match 1207 to 1497 in *T. thermophila* citrate synthase/14 nm filament protein (CS/14FP) mRNA (GenBank accession no. D90117) delineated below. Asterisks symbolize identity. The 5' 13-mer arbitrary primer and the 3' sequence complementary to the single-base-anchored oligo-dT₁₁ primer are underlined. A mismatch occurs at position 3. Both ends terminate with AAGCTT, a *Hind* III restriction site included in the primers. In-frame TGA stop codons are shaded beginning at position 193. Black dots mark a hexanucleotide poly(A) signal at positions 265 to 270 and a second poly(A) signal at positions 355 to 360. The sequence was identical in five independent clones, one of which was a complementary sequence. Technical details are in Appendices 1.6 to 1.9.

Fig. S6. Morphology of *T. thermophila* cells at 72 h of culture in late stationary phase. (A) Scanning electron microscopy (SEM) image of a typical vegetative cell. The cell body is teardrop shaped with its anterior end at top. Numerous cilia cover the external surface. The oral apparatus is prominently located left anterior. Scale bar equals 10

μm . (B-D, G and I) Phase-contrast micrographs of wet mounts of cells rapidly fixed in freshly mixed glutaraldehyde/osmium tetroxide. Scale bars equal 25 μm . (B) Inbred strain SB1969 cells exhibited a wide variety of teardrop shapes in a control culture. (C-I) FIR treated cultures. (C) Spindle shaped SB1969 cells, three bearing a caudal cilium that lies in a single focal plane (arrowheads). (D) A spindle shaped SB1969 cell with an inconspicuous slit-like aperture (large arrowhead) and a caudal cilium (small arrowhead). (E) SEM image of a similar cell with a cleft that might appear to be a slit-like aperture under phase-contrast microscopy. Scale bar equals 5 μm . (F) A close up view of the cleft. Scale bar equals 1 μm . (G) A roughly diamond shaped SB1969 cell with an emergent caudal cilium (arrowhead). (H) SEM image of another such diamond shaped cell. Scale bar equals 5 μm . (I) A slender spindle shaped SB210 cell with a caudal cilium (arrowhead). The images in panels B-D, G and I represent inspection of multiple fields from three independent experiments. Technical details are in Appendix 1.14.

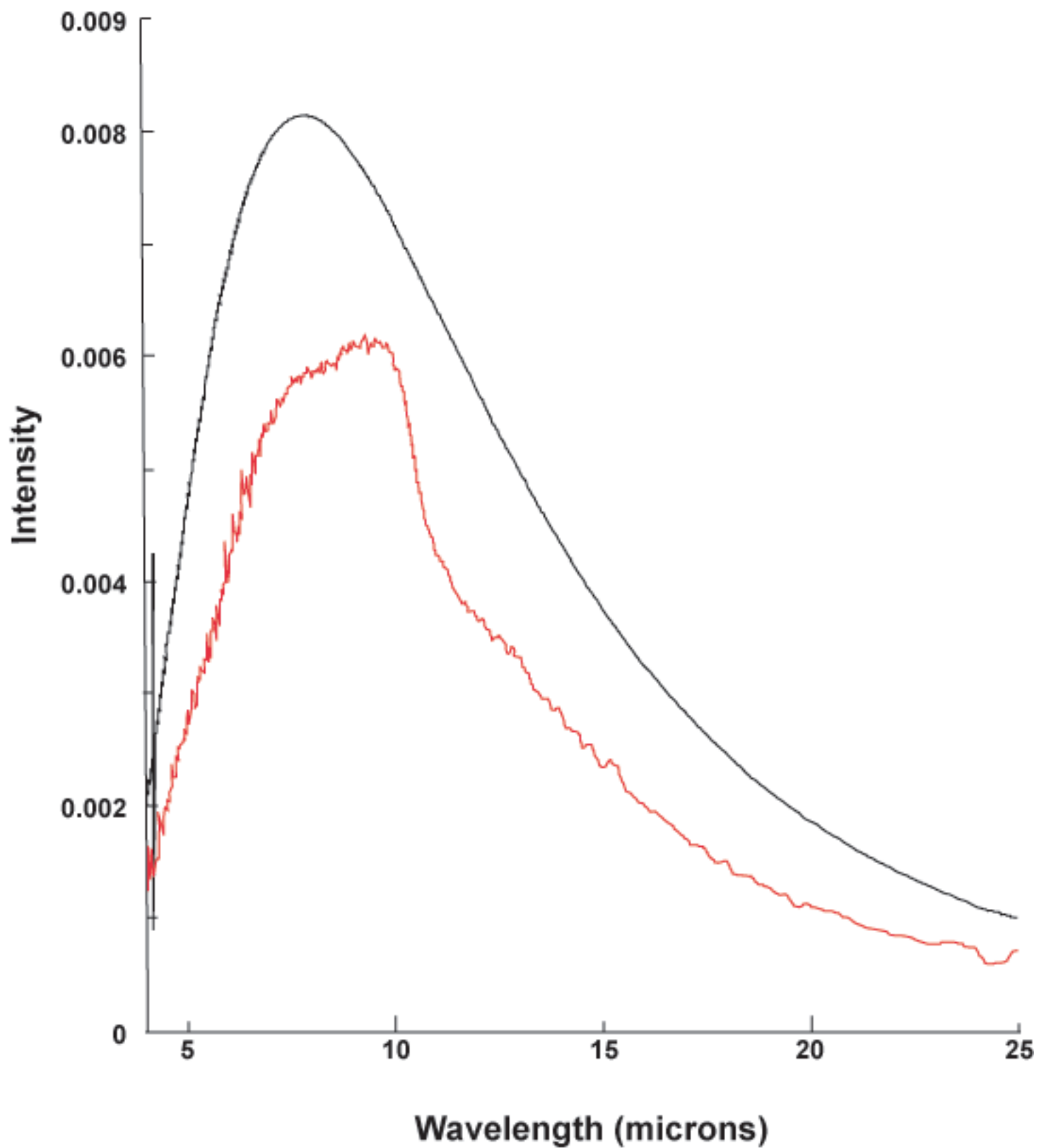


Fig. S1

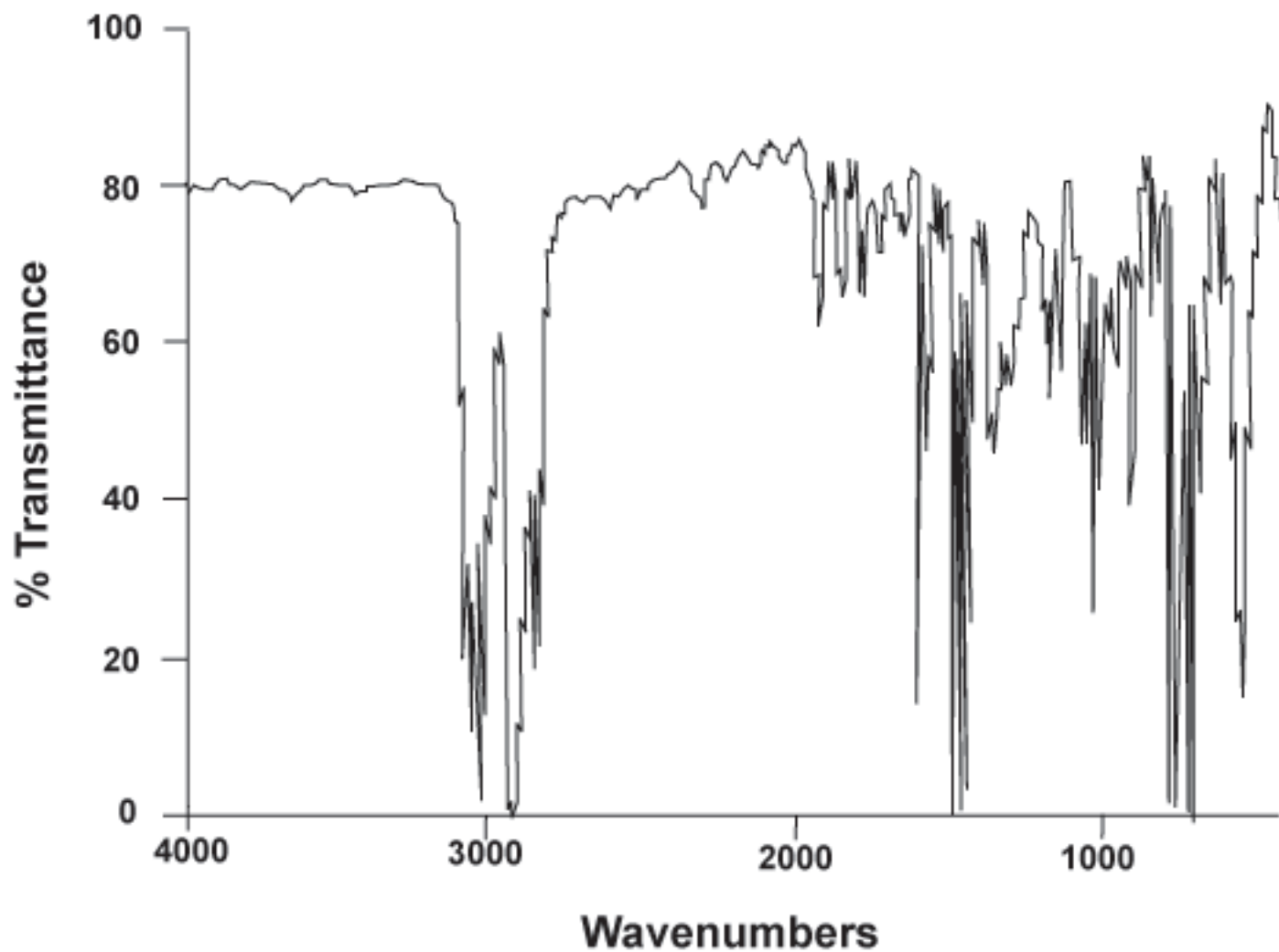


Fig. S2

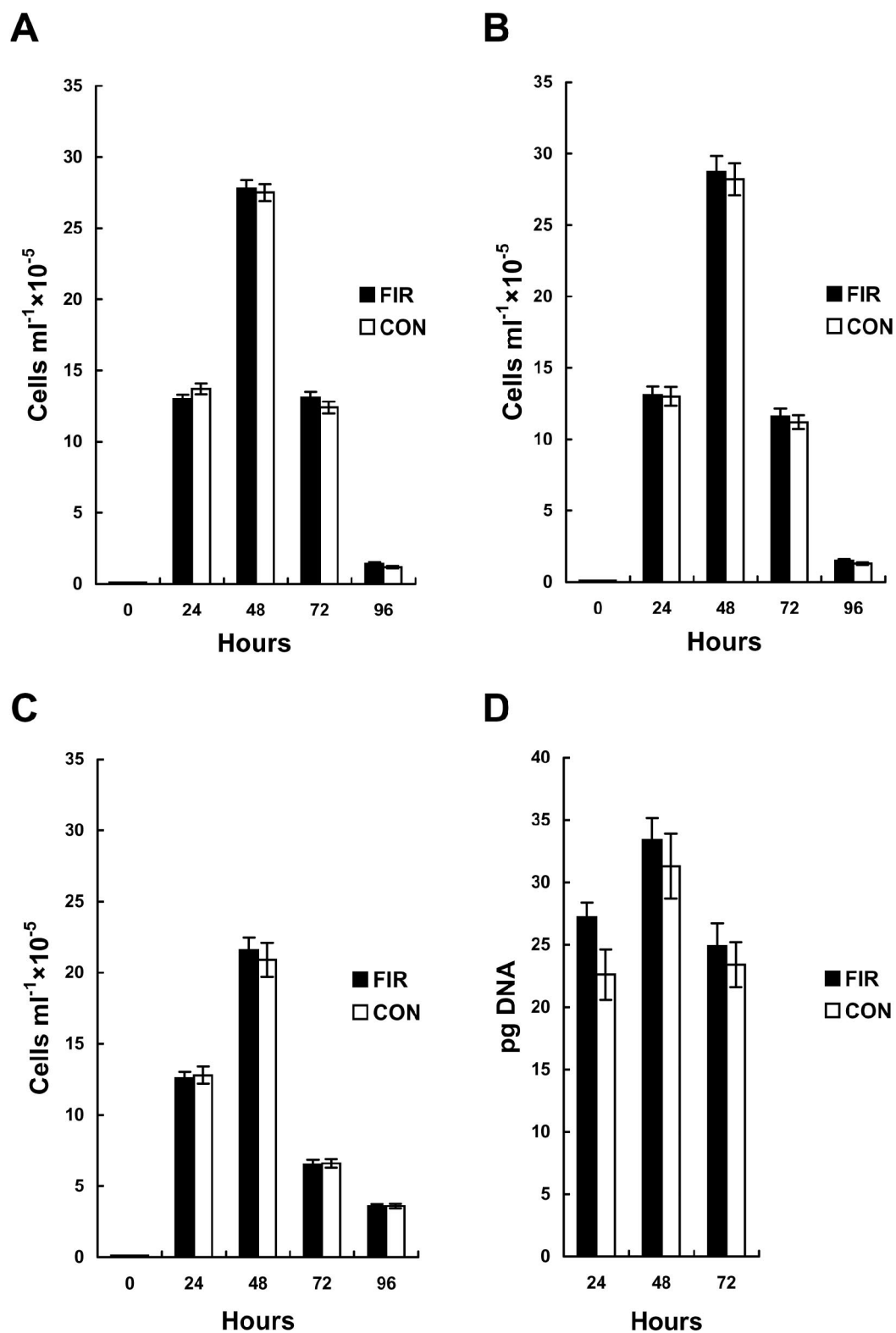


Fig. S3

FIR

Control

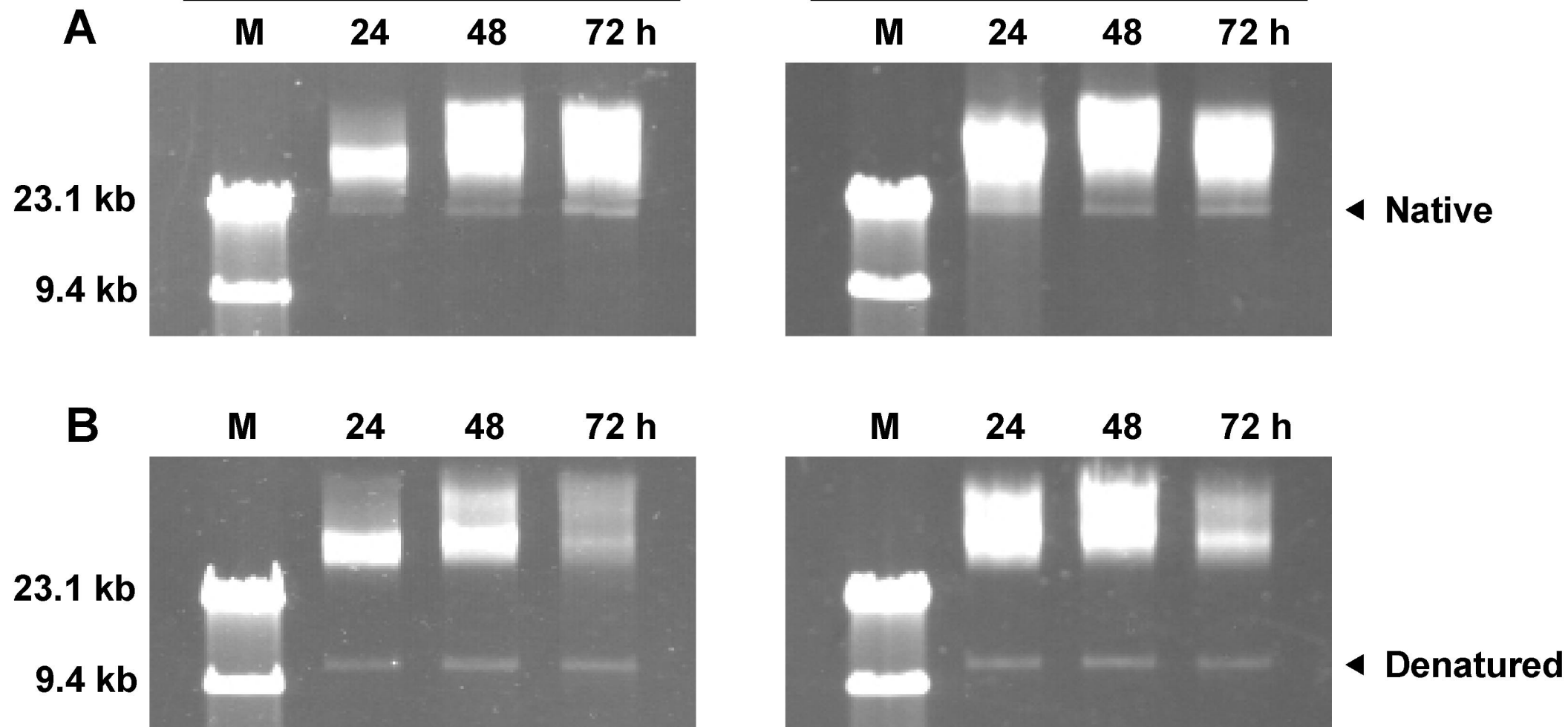
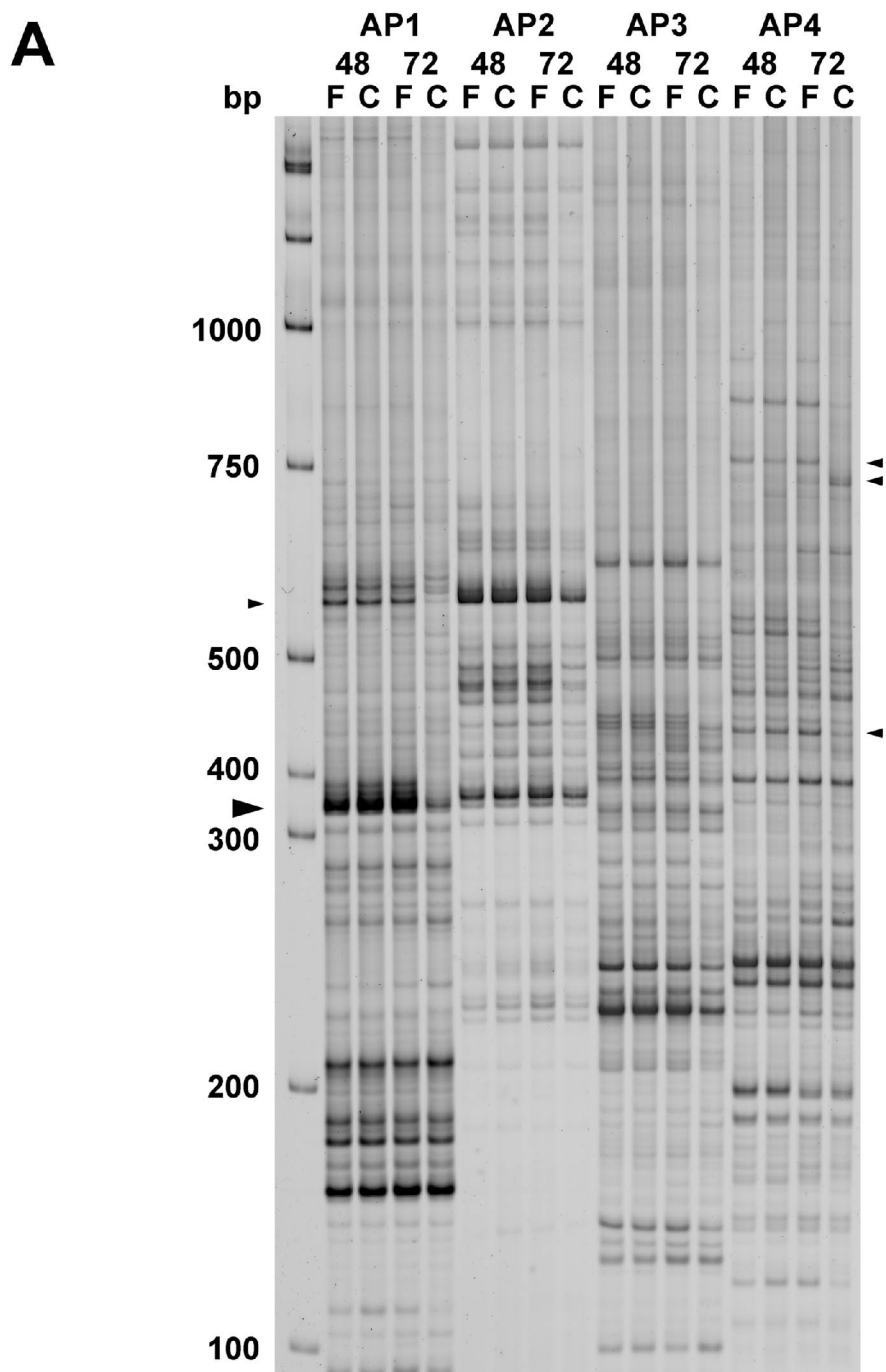


Fig. S4



B

	10	20	30	40	50
5'	<u>AAGCTT</u> GATT	GCCACTCTGG	TGTTTTATTA	TACTCTTTGG	GCTTAACTGA
	AATGTTGATT	GCC*****	*****	*****	*****
	60	70	80	90	100
	ATATCAATAT	TACACTGTTG	TCTTCGCCGT	TTCTAGAGCT	CTTGTTTGTA
	*****	*****	*****	*****	*****
	110	120	130	140	150
	TGGCTAACCT	CATCTGGTCT	AGAGCTTTCG	GTTTACCCAT	TGAAAGACCT
	*****	*****	*****	*****	*****
	160	170	180	190	200
	GGCTCTGCTG	ATCTTAAGTG	GTTCCACGAC	AAGTACAGAG	AATGAACAAA
	*****	*****	*****	*****	*****
	210	220	230	240	250
	<u>TTGAACTATA</u>	AATTATTACT	ACTCTAATAT	TATTTTCGTC	GATATAAATT
	*****	*****	*****	*****	*****
	260	270	280	290	300
	TCTAATTAGT	CTTTAATAAA	AGTTGTATCA	ATTCAACTAA	TATCAAAGCT
	*****	*****●●●●●	*****	*****	*****
	310	320	330	340	350
	TTATAATATT	TTGTGTCAGT	ATCAAATGAG	AAATATTAAT	AGTTTTCGACG
	360	370	380		
	ATTTAATAAAA	TAAAAAAAAA	<u>AAGCTT</u>		
	●●●●●		3'		

Fig. S5

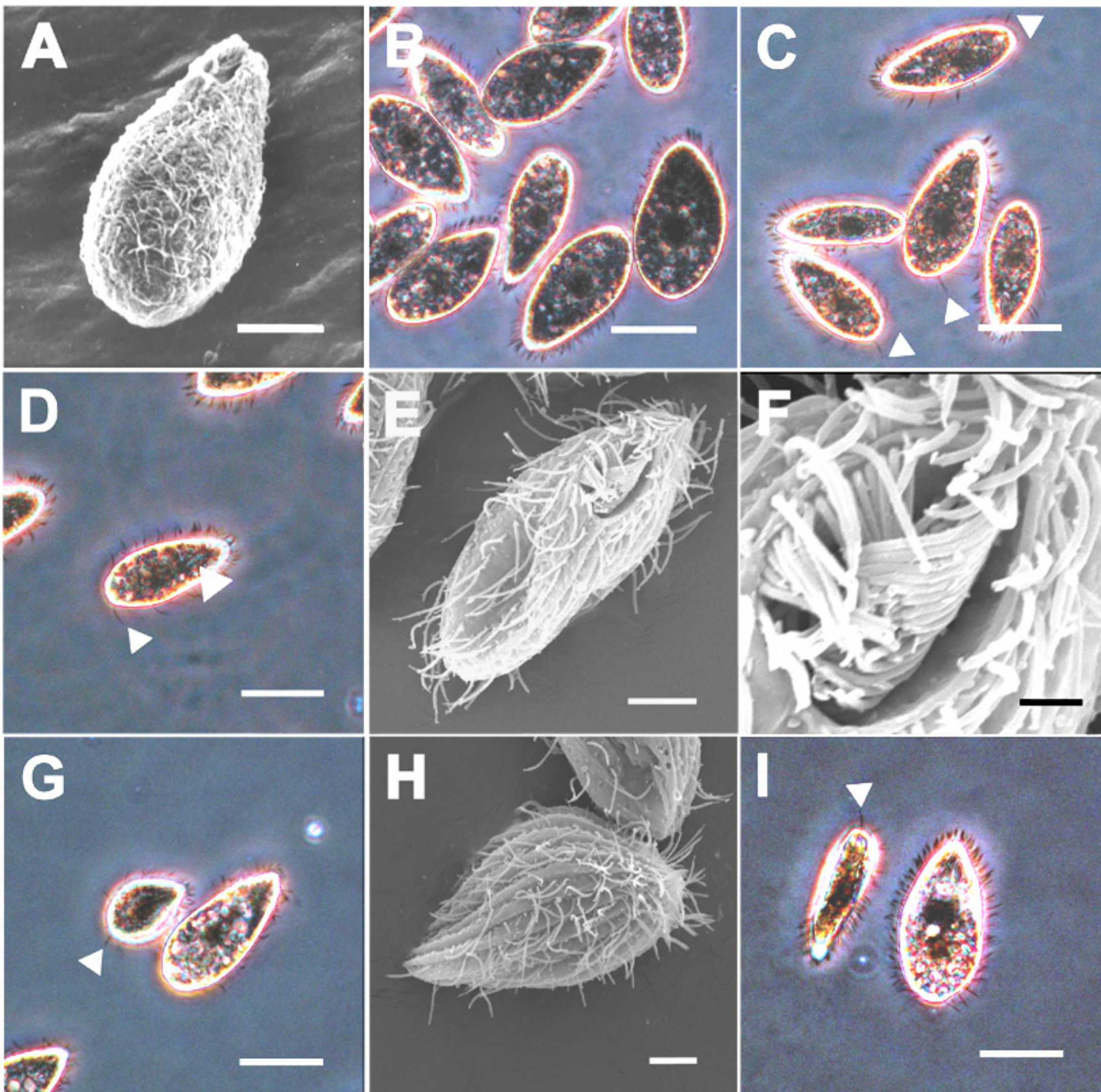


Fig. S6